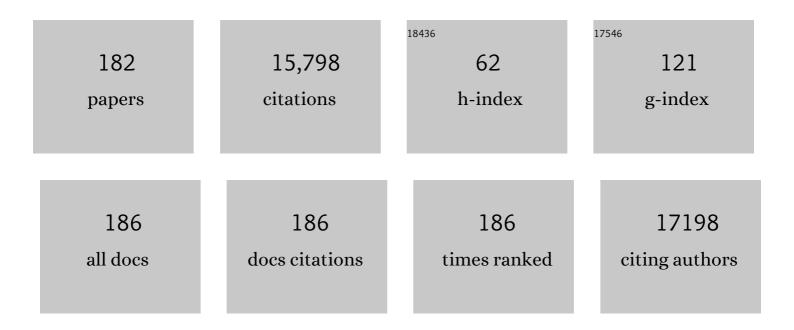
## Liang Chen

List of Publications by Year in descending order

Source: https://exaly.com/author-pdf/740878/publications.pdf Version: 2024-02-01



LIANC CHEN

#	Article	IF	CITATIONS
1	Towards Highâ€Voltage Aqueous Metalâ€Ion Batteries Beyond 1.5 V: The Zinc/Zinc Hexacyanoferrate System. Advanced Energy Materials, 2015, 5, 1400930.	10.2	932
2	Electrochemical Ammonia Synthesis via Nitrogen Reduction Reaction on a MoS <sub>2</sub> Catalyst: Theoretical and Experimental Studies. Advanced Materials, 2018, 30, e1800191.	11.1	697
3	Ternary Fe <sub><i>x</i></sub> Co <sub>1–<i>x</i></sub> P Nanowire Array as a Robust Hydrogen Evolution Reaction Electrocatalyst with Pt-like Activity: Experimental and Theoretical Insight. Nano Letters, 2016, 16, 6617-6621.	4.5	618
4	Enhanced Electrocatalysis for Energyâ€Efficient Hydrogen Production over CoP Catalyst with Nonelectroactive Zn as a Promoter. Advanced Energy Materials, 2017, 7, 1700020.	10.2	519
5	Boosted Electrocatalytic N <sub>2</sub> Reduction to NH <sub>3</sub> by Defectâ€Rich MoS <sub>2</sub> Nanoflower. Advanced Energy Materials, 2018, 8, 1801357.	10.2	482
6	Mn Doping of CoP Nanosheets Array: An Efficient Electrocatalyst for Hydrogen Evolution Reaction with Enhanced Activity at All pH Values. ACS Catalysis, 2017, 7, 98-102.	5.5	461
7	Promotional Effect of Ce-doped V <sub>2</sub> O <sub>5</sub> -WO <sub>3</sub> /TiO <sub>2</sub> with Low Vanadium Loadings for Selective Catalytic Reduction of NO <i><sub>x</sub></i> by NH <sub>3</sub> . Journal of Physical Chemistry C, 2009, 113, 21177-21184.	1.5	430
8	Chromium-ruthenium oxide solid solution electrocatalyst for highly efficient oxygen evolution reaction in acidic media. Nature Communications, 2019, 10, 162.	5.8	396
9	Assembling Ultrasmall Copperâ€Doped Ruthenium Oxide Nanocrystals into Hollow Porous Polyhedra: Highly Robust Electrocatalysts for Oxygen Evolution in Acidic Media. Advanced Materials, 2018, 30, e1801351.	11.1	353
10	Self‣tanding CoP Nanosheets Array: A Threeâ€Dimensional Bifunctional Catalyst Electrode for Overall Water Splitting in both Neutral and Alkaline Media. ChemElectroChem, 2017, 4, 1840-1845.	1.7	345
11	Metalâ€Organic Frameworks for Carbon Dioxide Capture and Methane Storage. Advanced Energy Materials, 2017, 7, 1601296.	10.2	334
12	A review of reproductive toxicity of microcystins. Journal of Hazardous Materials, 2016, 301, 381-399.	6.5	280
13	High-Performance Electrohydrogenation of N <sub>2</sub> to NH <sub>3</sub> Catalyzed by Multishelled Hollow Cr <sub>2</sub> O <sub>3</sub> Microspheres under Ambient Conditions. ACS Catalysis, 2018, 8, 8540-8544.	5.5	280
14	Al-Doped CoP nanoarray: a durable water-splitting electrocatalyst with superhigh activity. Nanoscale, 2017, 9, 4793-4800.	2.8	268
15	Global geographical and historical overview of cyanotoxin distribution and cyanobacterial poisonings. Archives of Toxicology, 2019, 93, 2429-2481.	1.9	230
16	Recent progress in single-atom electrocatalysts: concept, synthesis, and applications in clean energy conversion. Journal of Materials Chemistry A, 2018, 6, 14025-14042.	5.2	224
17	Theoretical Screening of Single Transition Metal Atoms Embedded in MXene Defects as Superior Electrocatalyst of Nitrogen Reduction Reaction. Small Methods, 2019, 3, 1900337.	4.6	213
18	Selective phosphidation: an effective strategy toward CoP/CeO <sub>2</sub> interface engineering for superior alkaline hydrogen evolution electrocatalysis. Journal of Materials Chemistry A, 2018, 6, 1985-1990.	5.2	212

#	Article	lF	CITATIONS
19	Morphology-Dependent Electrochemical Performance of Zinc Hexacyanoferrate Cathode for Zinc-Ion Battery. Scientific Reports, 2015, 5, 18263.	1.6	211
20	Direct synthesis of amine-functionalized MIL-101(Cr) nanoparticles and application for CO2 capture. RSC Advances, 2012, 2, 6417.	1.7	209
21	Largeâ€Sized Fewâ€Layer Graphene Enables an Ultrafast and Longâ€Life Aluminumâ€Ion Battery. Advanced Energy Materials, 2017, 7, 1700034.	10.2	197
22	In situ formation of a 3D core/shell structured Ni <sub>3</sub> N@Ni–Bi nanosheet array: an efficient non-noble-metal bifunctional electrocatalyst toward full water splitting under near-neutral conditions. Journal of Materials Chemistry A, 2017, 5, 7806-7810.	5.2	196
23	Soybean miR172c Targets the Repressive AP2 Transcription Factor NNC1 to Activate <i>ENOD40</i> Expression and Regulate Nodule Initiation Â. Plant Cell, 2015, 26, 4782-4801.	3.1	188
24	MicroRNA167-Directed Regulation of the Auxin Response Factors <i>GmARF8a</i> and <i>GmARF8b</i> Is Required for Soybean Nodulation and Lateral Root Development. Plant Physiology, 2015, 168, 984-999.	2.3	183
25	Ultrafine Defective RuO <sub>2</sub> Electrocatayst Integrated on Carbon Cloth for Robust Water Oxidation in Acidic Media. Advanced Energy Materials, 2019, 9, 1901313.	10.2	182
26	Global transcriptome and gene regulation network for secondary metabolite biosynthesis of tea plant (Camellia sinensis). BMC Genomics, 2015, 16, 560.	1.2	174
27	Amine-functionalized metal–organic frameworks: structure, synthesis and applications. RSC Advances, 2016, 6, 32598-32614.	1.7	169
28	Fabricating Singleâ€Atom Catalysts from Chelating Metal in Open Frameworks. Advanced Materials, 2019, 31, e1808193.	11.1	153
29	TRIM25 promotes the cell survival and growth of hepatocellular carcinoma through targeting Keap1-Nrf2 pathway. Nature Communications, 2020, 11, 348.	5.8	150
30	Self-supported CoMoS4 nanosheet array as an efficient catalyst for hydrogen evolution reaction at neutral pH. Nano Research, 2018, 11, 2024-2033.	5.8	147
31	A Ni(OH) <sub>2</sub> –PtO <sub>2</sub> hybrid nanosheet array with ultralow Pt loading toward efficient and durable alkaline hydrogen evolution. Journal of Materials Chemistry A, 2018, 6, 1967-1970.	5.2	134
32	Hydrogen spillover in the context of hydrogen storage using solid-state materials. Energy and Environmental Science, 2008, 1, 338.	15.6	133
33	Ammonia Thermal Treatment toward Topological Defects in Porous Carbon for Enhanced Carbon Dioxide Electroreduction. Advanced Materials, 2020, 32, e2001300.	11.1	130
34	Hydrogen Absorption and Diffusion in Bulk α-MoO <sub>3</sub> . Journal of Physical Chemistry C, 2009, 113, 11399-11407.	1.5	126
35	A Co-Doped Nanorod-like RuO2 Electrocatalyst with Abundant Oxygen Vacancies for Acidic Water Oxidation. IScience, 2020, 23, 100756.	1.9	125
36	Hexagonal boron nitride nanosheet for effective ambient N2 fixation to NH3. Nano Research, 2019, 12, 919-924.	5.8	120

#	Article	IF	CITATIONS
37	Facile synthesis of Fe-MOF/RGO and its application as a high performance anode in lithium-ion batteries. RSC Advances, 2016, 6, 30763-30768.	1.7	118
38	A self-supported NiMoS <sub>4</sub> nanoarray as an efficient 3D cathode for the alkaline hydrogen evolution reaction. Journal of Materials Chemistry A, 2017, 5, 16585-16589.	5.2	114
39	Atomically dispersed Lewis acid sites boost 2-electron oxygen reduction activity of carbon-based catalysts. Nature Communications, 2020, 11, 5478.	5.8	114
40	Responses of the Proteome and Metabolome in Livers of Zebrafish Exposed Chronically to Environmentally Relevant Concentrations of Microcystin-LR. Environmental Science & Technology, 2017, 51, 596-607.	4.6	109
41	The Critical Role of Additive Sulfate for Stable Alkaline Seawater Oxidation on Nickelâ€Based Electrodes. Angewandte Chemie - International Edition, 2021, 60, 22740-22744.	7.2	108
42	On the Mechanisms of Hydrogen Spillover in MoO <sub>3</sub> . Journal of Physical Chemistry C, 2008, 112, 1755-1758.	1.5	98
43	Challenges of using blooms of Microcystis spp. in animal feeds: A comprehensive review of nutritional, toxicological and microbial health evaluation. Science of the Total Environment, 2021, 764, 142319.	3.9	97
44	Bimetallic Nickelâ€Substituted Cobaltâ€Borate Nanowire Array: An Earthâ€Abundant Water Oxidation Electrocatalyst with Superior Activity and Durability at Near Neutral pH. Small, 2017, 13, 1700394.	5.2	95
45	Nanoscale MOF/organosilica membranes on tubular ceramic substrates for highly selective gas separation. Energy and Environmental Science, 2017, 10, 1812-1819.	15.6	95
46	Biochemical and transcriptomic analyses reveal different metabolite biosynthesis profiles among three color and developmental stages in â€~Anji Baicha' (Camellia sinensis). BMC Plant Biology, 2016, 16, 195.	1.6	93
47	New-concept Batteries Based on Aqueous Li+/Na+ Mixed-ion Electrolytes. Scientific Reports, 2013, 3, 1946.	1.6	91
48	Water-mediated cation intercalation of open-framework indium hexacyanoferrate with high voltage and fast kinetics. Nature Communications, 2016, 7, 11982.	5.8	90
49	Theoretical Investigation on the Single Transition-Metal Atom-Decorated Defective MoS <sub>2</sub> for Electrocatalytic Ammonia Synthesis. ACS Applied Materials & Interfaces, 2019, 11, 36506-36514.	4.0	88
50	Methylsulfonylmethane-Based Deep Eutectic Solvent as a New Type of Green Electrolyte for a High-Energy-Density Aqueous Lithium-Ion Battery. ACS Energy Letters, 2019, 4, 1419-1426.	8.8	87
51	Recent Progress in Low Pt Content Electrocatalysts for Hydrogen Evolution Reaction. Advanced Materials Interfaces, 2020, 7, 2000396.	1.9	84
52	Tunable electronic and magnetic properties of Cr2M′C2T2 (M′ = Ti or V; T = O, OH or F) Letters, 2016, 109, .	. Applied P	'hysics
53	Trace elements in fish from Taihu Lake, China: Levels, associated risks, and trophic transfer. Ecotoxicology and Environmental Safety, 2013, 90, 89-97.	2.9	80
54	Efficient Hydrogen Evolution Electrocatalysis at Alkaline pH by Interface Engineering of	1.9	78

Efficient Hydrogen Evolution Electrocatalysis at Alkaline pH by Interface Engineering of Ni<sub>2</sub>P–CeO<sub>2</sub>. Inorganic Chemistry, 2018, 57, 548-552. 54

#	Article	IF	CITATIONS
55	Construction of a SSR-Based Genetic Map and Identification of QTLs for Catechins Content in Tea Plant (Camellia sinensis). PLoS ONE, 2014, 9, e93131.	1.1	75
56	Mechanisms of Microcystin-induced Cytotoxicity and Apoptosis. Mini-Reviews in Medicinal Chemistry, 2016, 16, 1018-1031.	1.1	75
57	Ion-selective copper hexacyanoferrate with an open-framework structure enables high-voltage aqueous mixed-ion batteries. Journal of Materials Chemistry A, 2017, 5, 16740-16747.	5.2	74
58	Kinetically Stabilized Pd@Pt Core–Shell Octahedral Nanoparticles with Thin Pt Layers for Enhanced Catalytic Hydrogenation Performance. ACS Catalysis, 2015, 5, 1335-1343.	5.5	72
59	Atomically Dispersed Highâ€Density Al–N <sub>4</sub> Sites in Porous Carbon for Efficient Photodriven CO <sub>2</sub> Cycloaddition. Advanced Materials, 2021, 33, e2103186.	11.1	69
60	Large-Scale SNP Discovery and Genotyping for Constructing a High-Density Genetic Map of Tea Plant Using Specific-Locus Amplified Fragment Sequencing (SLAF-seq). PLoS ONE, 2015, 10, e0128798.	1.1	68
61	Involvement of oxidative stress and cytoskeletal disruption in microcystin-induced apoptosis in CIK cells. Aquatic Toxicology, 2015, 165, 41-50.	1.9	67
62	Si/Ag/C Nanohybrids with <i>in Situ</i> Incorporation of Super-Small Silver Nanoparticles: Tiny Amount, Huge Impact. ACS Nano, 2018, 12, 861-875.	7.3	67
63	Phase-selective synthesis of self-supported RuP films for efficient hydrogen evolution electrocatalysis in alkaline media. Nanoscale, 2018, 10, 13930-13935.	2.8	67
64	Transcriptomic Analysis of Tea Plant Responding to Drought Stress and Recovery. PLoS ONE, 2016, 11, e0147306.	1.1	67
65	Aqueous Batteries Based on Mixed Monovalence Metal Ions: A New Battery Family. ChemSusChem, 2014, 7, 2295-2302.	3.6	61
66	A hollow ceramic fiber supported ZIF-8 membrane with enhanced gas separation performance prepared by hot dip-coating seeding. Journal of Materials Chemistry A, 2013, 1, 13046.	5.2	60
67	Female zebrafish (Danio rerio) are more vulnerable than males to microcystin-LR exposure, without exhibiting estrogenic effects. Aquatic Toxicology, 2013, 142-143, 272-282.	1.9	60
68	High-Throughput Screening of a Single-Atom Alloy for Electroreduction of Dinitrogen to Ammonia. ACS Applied Materials & Interfaces, 2021, 13, 16336-16344.	4.0	58
69	Genome-Wide Small RNA Analysis of Soybean Reveals Auxin-Responsive microRNAs that are Differentially Expressed in Response to Salt Stress in Root Apex. Frontiers in Plant Science, 2015, 6, 1273.	1.7	57
70	Natural allelic variations of TCS1 play a crucial role in caffeine biosynthesis of tea plant and its related species. Plant Physiology and Biochemistry, 2016, 100, 18-26.	2.8	56
71	Benzoate Anionâ€Intercalated Layered Cobalt Hydroxide Nanoarray: An Efficient Electrocatalyst for the Oxygen Evolution Reaction. ChemSusChem, 2017, 10, 4004-4008.	3.6	56
72	Enhancement of Mass Transfer for Facilitating Industrial‣evel CO <sub>2</sub> Electroreduction on Atomic NiN <sub>4</sub> Sites. Advanced Energy Materials, 2021, 11, 2102152.	10.2	56

#	Article	IF	CITATIONS
73	Metalâ€Organic Frameworksâ€Derived Porous In <sub>2</sub> O <sub>3</sub> Hollow Nanorod for Highâ€Performance Ethanol Gas Sensor. ChemistrySelect, 2017, 2, 10918-10925.	0.7	55
74	Identification of Cold-Responsive miRNAs and Their Target Genes in Nitrogen-Fixing Nodules of Soybean. International Journal of Molecular Sciences, 2014, 15, 13596-13614.	1.8	54
75	Quantitative Succinyl-Proteome Profiling of Camellia sinensis cv. â€~Anji Baicha' During Periodic Albinism. Scientific Reports, 2017, 7, 1873.	1.6	54
76	The Critical Role of Additive Sulfate for Stable Alkaline Seawater Oxidation on Nickelâ€Based Electrodes. Angewandte Chemie, 2021, 133, 22922-22926.	1.6	53
77	Particle size studies to reveal crystallization mechanisms of the metal organic framework HKUST-1 during sonochemical synthesis. Ultrasonics Sonochemistry, 2017, 34, 365-370.	3.8	52
78	Small <scp>RNA</scp> and degradome profiling reveals important roles for <scp>microRNAs</scp> and their targets in tea plant response to drought stress. Physiologia Plantarum, 2016, 158, 435-451.	2.6	51
79	Comprehensive Dissection of Metabolic Changes in Albino and Green Tea Cultivars. Journal of Agricultural and Food Chemistry, 2018, 66, 2040-2048.	2.4	51
80	Recent Progress in the Theoretical Investigation of Electrocatalytic Reduction of CO <sub>2</sub> . Advanced Theory and Simulations, 2018, 1, 1800004.	1.3	50
81	GmYUC2a mediates auxin biosynthesis during root development and nodulation in soybean. Journal of Experimental Botany, 2019, 70, 3165-3176.	2.4	49
82	Designed Synthesis of Functionalized Twoâ€Dimensional Metal–Organic Frameworks with Preferential CO <sub>2</sub> Capture. ChemPlusChem, 2013, 78, 86-91.	1.3	48
83	Selfâ€Templating Construction of Hollow Amorphous CoMoS <sub>4</sub> Nanotube Array towards Efficient Hydrogen Evolution Electrocatalysis at Neutral pH. Chemistry - A European Journal, 2017, 23, 12718-12723.	1.7	48
84	The Interactive Effects of Cytoskeleton Disruption and Mitochondria Dysfunction Lead to Reproductive Toxicity Induced by Microcystin-LR. PLoS ONE, 2013, 8, e53949.	1.1	48
85	The use of RAPD markers for detecting genetic diversity, relationship and molecular identification of Chinese elite tea genetic resources [Camellia sinensis (L.) O. Kuntze] preserved in a tea germplasm repository. Biodiversity and Conservation, 2005, 14, 1433-1444.	1.2	47
86	The role of <scp>CSH</scp> in microcystinâ€induced apoptosis in rat liver: Involvement of oxidative stress and <scp>NF</scp> â€i <sup>®</sup> <scp>B</scp> . Environmental Toxicology, 2016, 31, 552-560.	2.1	47
87	Recent Advances in Metalâ€Organic Frameworks and Their Derived Materials for Electrocatalytic Water Splitting. ChemElectroChem, 2020, 7, 1805-1824.	1.7	47
88	Transitional Metal Catalytic Pyrite Cathode Enables Ultrastable Four-Electron-Based All-Solid-State Lithium Batteries. ACS Nano, 2019, 13, 9551-9560.	7.3	46
89	Microcystin-LR affects the hypothalamic-pituitary-inter-renal (HPI) axis in early life stages (embryos) Tj ETQq1	1 0.784314	rgBT /Overloo 45
90	Spatial and interspecies differences in concentrations of eight trace elements in wild freshwater fishes at different trophic levels from middle and eastern China. Science of the Total Environment, 2019, 672, 883-892.	3.9	45

#	Article	IF	CITATIONS
91	Topotactic Conversion of α-Fe <sub>2</sub> O <sub>3</sub> Nanowires into FeP as a Superior Fluorosensor for Nucleic Acid Detection: Insights from Experiment and Theory. Analytical Chemistry, 2017, 89, 2191-2195.	3.2	44
92	Differential Metabolic Profiles during the Albescent Stages of â€~Anji Baicha' (Camellia sinensis). PLoS ONE, 2015, 10, e0139996.	1.1	43
93	Threeâ€Dimensional Nickel–Borate Nanosheets Array for Efficient Oxygen Evolution at Nearâ€Neutral pH. Chemistry - A European Journal, 2017, 23, 6959-6963.	1.7	43
94	The dose makes the poison. Science of the Total Environment, 2018, 621, 649-653.	3.9	43
95	Cr <sub>3</sub> C <sub>2</sub> Nanoparticle-Embedded Carbon Nanofiber for Artificial Synthesis of NH <sub>3</sub> through N <sub>2</sub> Fixation under Ambient Conditions. ACS Applied Materials & amp; Interfaces, 2019, 11, 35764-35769.	4.0	43
96	Identification and expression profiling of the auxin response factors (ARFs) in the tea plant (Camellia) Tj ETQq0 0 46-56.	0 rgBT /O 2.8	verlock 10 Tf 42
97	Polyethylene Glycol–Na <sup>+</sup> Interface of Vanadium Hexacyanoferrate Cathode for Highly Stable Rechargeable Aqueous Sodium-Ion Battery. ACS Applied Materials & Interfaces, 2019, 11, 28762-28768.	4.0	41
98	Differential Permeability of Proton Isotopes through Graphene and Graphene Analogue Monolayer. Journal of Physical Chemistry Letters, 2016, 7, 3395-3400.	2.1	40
99	Co-based nanowire films as complementary hydrogen- and oxygen-evolving electrocatalysts in neutral electrolyte. Catalysis Science and Technology, 2017, 7, 2689-2694.	2.1	39
100	Farmland heavy metals can migrate to deep soil at a regional scale: A case study on a wastewater-irrigated area in China. Environmental Pollution, 2021, 281, 116977.	3.7	39
101	Transcriptome and metabolome analysis reveal candidate genes and biochemicals involved in tea geometrid defense in Camellia sinensis. PLoS ONE, 2018, 13, e0201670.	1.1	38
102	Sex-dependent effects of microcystin-LR on hypothalamic-pituitary-gonad axis and gametogenesis of adult zebrafish. Scientific Reports, 2016, 6, 22819.	1.6	37
103	Insights into High Conductivity of the Two-Dimensional Iodine-Oxidized sp <sup>2</sup> -c-COF. ACS Applied Materials & Interfaces, 2018, 10, 43595-43602.	4.0	37
104	Mg-Doping improves the performance of Ru-based electrocatalysts for the acidic oxygen evolution reaction. Chemical Communications, 2020, 56, 1749-1752.	2.2	36
105	Promoting effects of Ce <sub>0.75</sub> Zr <sub>0.25</sub> O <sub>2</sub> on the La <sub>0.7</sub> Sr <sub>0.3</sub> MnO <sub>3</sub> electrocatalyst for the oxygen reduction reaction in metal–air batteries. Journal of Materials Chemistry A, 2017, 5, 6411-6415.	5.2	35
106	NF-κB plays a key role in microcystin-RR-induced HeLa cell proliferation and apoptosis. Toxicon, 2014, 87, 120-130.	0.8	34
107	Proteome and Acetyl-Proteome Profiling of Camellia sinensis cv. â€~Anji Baicha' during Periodic Albinism Reveals Alterations in Photosynthetic and Secondary Metabolite Biosynthetic Pathways. Frontiers in Plant Science, 2017, 8, 2104.	1.7	33
108	Catalyzed activation of CO2 by a Lewis-base site in W–Cu–BTC hybrid metal organic frameworks. Chemical Science, 2012, 3, 2708.	3.7	32

#	Article	IF	CITATIONS
109	Seasonal Dynamics in Resource Partitioning to Growth and Storage in Response to Drought in a Perennial Rhizomatous Grass, Leymus chinensis. Journal of Plant Growth Regulation, 2008, 27, 39-48.	2.8	31
110	n-Octadecanethiol self-assembled monolayer coating with microscopic roughness for dropwise condensation of steam. Journal of Thermal Science, 2009, 18, 160-165.	0.9	31
111	Quantitatively evaluating detoxification of the hepatotoxic microcystin-LR through the glutathione (GSH) pathway in SD rats. Environmental Science and Pollution Research, 2015, 22, 19273-19284.	2.7	30
112	Cobalt-Borate Nanoarray: An Efficient and Durable Electrocatalyst for Water Oxidation under Benign Conditions. ACS Applied Materials & Interfaces, 2017, 9, 15383-15387.	4.0	30
113	Functional natural allelic variants of flavonoid 3′,5′-hydroxylase gene governing catechin traits in tea plant and its relatives. Planta, 2017, 245, 523-538.	1.6	30
114	Bioaccumulation and human health risk assessment of trace metals in the freshwater mussel Cristaria plicata in Dongting Lake, China. Journal of Environmental Sciences, 2021, 104, 335-350.	3.2	30
115	Effects of acute exposure to microcystins on hypothalamic-pituitary-adrenal (HPA), -gonad (HPG) and -thyroid (HPT) axes of female rats. Science of the Total Environment, 2021, 778, 145196.	3.9	29
116	Ligand Defect Density Regulation in Metal–Organic Frameworks by Functional Group Engineering on Linkers. Nano Letters, 2022, 22, 838-845.	4.5	29
117	Association mapping of caffeine content with TCS1 in tea plant and its related species. Plant Physiology and Biochemistry, 2016, 105, 251-259.	2.8	28
118	The role of glutathione detoxification pathway in MCLR-induced hepatotoxicity in SD rats. Environmental Toxicology, 2015, 30, 1470-1480.	2.1	27
119	Hydrogen adsorption and desorption on the Pt and Pd subnano clusters — a review. Frontiers of Physics in China, 2009, 4, 356-366.	1.0	26
120	Molecular simulation of CO <sub>2</sub> , N <sub>2</sub> and CH <sub>4</sub> adsorption and separation in ZIF-78 and ZIF-79. Molecular Simulation, 2011, 37, 1131-1142.	0.9	26
121	Quantitative Trait Loci Mapping for Theobromine and Caffeine Contents in Tea Plant ( <i>Camellia) Tj ETQq1 1 0</i>	.784314 r 2.4	gBT /Overloc 26
122	Dental Resin Monomer Enables Unique NbO <sub>2</sub> /Carbon Lithiumâ€lon Battery Negative Electrode with Exceptional Performance. Advanced Functional Materials, 2019, 29, 1904961.	7.8	26
123	Double Atom Catalysts: Heteronuclear Transition Metal Dimer Anchored on Nitrogenâ€Đoped Graphene as Superior Electrocatalyst for Nitrogen Reduction Reaction. Advanced Theory and Simulations, 2020, 3, 2000190.	1.3	26
124	Integrative plasma proteomic and microRNA analysis of Jersey cattle in response to high-altitude hypoxia. Journal of Dairy Science, 2019, 102, 4606-4618.	1.4	25
125	Monitoring graphene oxide's efficiency for removing Re(VII) and Cr(VI) with fluorescent silica hydrogels. Environmental Pollution, 2020, 262, 114246.	3.7	25
126	Sol–gel auto-combustion synthesis of Ni–CexZr1â^'xO2 catalysts for carbon dioxide reforming of methane. RSC Advances, 2013, 3, 22285.	1.7	24

#	Article	IF	CITATIONS
127	Visible/infrared light-driven high-efficiency CO <sub>2</sub> conversion into ethane based on a B–Co synergistic catalyst. Journal of Materials Chemistry A, 2020, 8, 22327-22334.	5.2	24
128	Fast and Stable Electrochemical Production of H <sub>2</sub> O <sub>2</sub> by Electrode Architecture Engineering. ACS Sustainable Chemistry and Engineering, 2021, 9, 7120-7129.	3.2	24
129	A NbO type microporous metal–organic framework constructed from a naphthalene derived ligand for CH <sub>4</sub> and C <sub>2</sub> H <sub>2</sub> storage at room temperature. RSC Advances, 2014, 4, 49457-49461.	1.7	23
130	Integrating PtNi nanoparticles on NiFe layered double hydroxide nanosheets as a bifunctional catalyst for hybrid sodium–air batteries. Journal of Materials Chemistry A, 2020, 8, 16355-16365.	5.2	21
131	Health Risks of Chronic Exposure to Small Doses of Microcystins: An Integrative Metabolomic and Biochemical Study of Human Serum. Environmental Science & Technology, 2022, 56, 6548-6559.	4.6	21
132	Compositional and Morphological Changes of Ordered Pt <sub><i>x</i></sub> Fe <sub><i>y</i></sub> /C Oxygen Electroreduction Catalysts. ChemCatChem, 2013, 5, 1449-1460.	1.8	20
133	Surface Modifications of Ti <sub>2</sub> CO <sub>2</sub> for Obtaining High Hydrogen Evolution Reaction Activity and Conductivity: A Computational Approach. ChemPhysChem, 2018, 19, 3380-3387.	1.0	20
134	Emerging Roles of Tripartite Motif-Containing Family Proteins (TRIMs) in Eliminating Misfolded Proteins. Frontiers in Cell and Developmental Biology, 2020, 8, 802.	1.8	20
135	Origin of Rh and Pd agglomeration on the <mml:math xmlns:mml="http://www.w3.org/1998/Math/MathML" display="inline"&gt;<mml:mrow><mml:mrow><mml:mtext>CeO</mml:mtext></mml:mrow><mml:m Physical Review B, 2010, 82, .</mml:m </mml:mrow></mml:math 	n>2 <sup>1,1</sup> /mml	:mn>
136	MOFâ€Derived Zincâ€Doped Ruthenium Oxide Hollow Nanorods as Highly Active and Stable Electrocatalysts for Oxygen Evolution in Acidic Media. ChemNanoMat, 2021, 7, 117-121.	1.5	18
137	Multi-Omics Analysis Reveals Up-Regulation of APR Signaling, LXR/RXR and FXR/RXR Activation Pathways in Holstein Dairy Cows Exposed to High-Altitude Hypoxia. Animals, 2019, 9, 406.	1.0	17
138	Theoretical Understanding of the Interface Effect in Promoting Electrochemical CO <sub>2</sub> Reduction on Cu–Pd Alloys. Journal of Physical Chemistry C, 2021, 125, 21381-21389.	1.5	17
139	Ultrathin Reduced Graphene Oxide/Organosilica Hybrid Membrane for Gas Separation. Jacs Au, 2021, 1, 328-335.	3.6	16
140	Quantitative liquid chromatography–tandem mass spectrometry method for determination of microcystin-RR and its glutathione and cysteine conjugates in fish plasma and bile. Journal of Chromatography B: Analytical Technologies in the Biomedical and Life Sciences, 2014, 963, 113-118.	1.2	15
141	Synergistic Tumor Cytolysis by NK Cells in Combination With a Pan-HDAC Inhibitor, Panobinostat. Frontiers in Immunology, 2021, 12, 701671.	2.2	15
142	Ultrathin-Nanosheets-Composed CoSP Nanobrushes as an All-pH Highly Efficient Catalyst toward Hydrogen Evolution. ACS Sustainable Chemistry and Engineering, 2018, 6, 15618-15623.	3.2	14
143	Isolation and Characterization of CsWRKY7, a Subgroup IId WRKY Transcription Factor from Camellia sinensis, Linked to Development in Arabidopsis. International Journal of Molecular Sciences, 2019, 20, 2815.	1.8	14
144	TRIM11 cooperates with HSF1 to suppress the anti-tumor effect of proteotoxic stress drugs. Cell Cycle, 2019, 18, 60-68.	1.3	14

#	Article	IF	CITATIONS
145	<i>LHPP</i> inhibits hepatocellular carcinoma cell growth and metastasis. Cell Cycle, 2020, 19, 1846-1854.	1.3	14
146	Metagenomics-Guided Discovery of Potential Bacterial Metallothionein Genes from the Soil Microbiome That Confer Cu and/or Cd Resistance. Applied and Environmental Microbiology, 2020, 86, .	1.4	14
147	Recent advances on electrocatalytic fixation of nitrogen under ambient conditions. Materials Chemistry Frontiers, 2021, 5, 5516-5533.	3.2	14
148	A Joint Theoretical and Experimental Study of Phase Equilibria and Evolution in Pt-Doped Calcium Titanate under Redox Conditions. Chemistry of Materials, 2015, 27, 18-28.	3.2	13
149	A molecular-templating strategy to polyamine-incorporated porous organic polymers for unprecedented CO2 capture and separation. Science China Materials, 2019, 62, 448-454.	3.5	13
150	A natural product, Piperlongumine (PL), increases tumor cells sensitivity to NK cell killing. International Immunopharmacology, 2021, 96, 107658.	1.7	13
151	A <sub><i>m</i></sub> V <sub>2</sub> O <sub>5</sub> with Binary Phases as High-Performance Cathode Materials for Zinc-Ion Batteries: Effect of the Pre-Intercalated Cations A and Reversible Transformation of Coordination Polyhedra. ACS Applied Materials & amp; Interfaces, 2022, 14, 24415-24424.	4.0	13
152	A mechanistic study of hydrogen spillover in MoO <sub>3</sub> and carbon-based graphitic materials. Journal of Physics Condensed Matter, 2008, 20, 064223.	0.7	12
153	Spin-flip phenomena at the Co graphene Co interfaces. Applied Physics Letters, 2011, 98, .	1.5	12
154	A newly-isolated Cd-loving Purpureocillium sp. strain YZ1 substantially alleviates Cd toxicity to wheat. Plant and Soil, 2021, 464, 289.	1.8	12
155	Enhanced catalytic performance of Pt by coupling with carbon defects. Innovation(China), 2021, 2, 100161.	5.2	11
156	Theoretical investigation of defective MXenes as potential electrocatalysts for CO reduction toward C <sub>2</sub> products. Physical Chemistry Chemical Physics, 2021, 23, 12431-12438.	1.3	11
157	Surface-termination-dependent Pd bonding and aggregation of nanoparticles on LaFeO3 (001). Journal of Chemical Physics, 2013, 138, 144705.	1.2	10
158	Two-dimensional semiconducting gold. Physical Review B, 2017, 95, .	1.1	10
159	Analysis of Genetic Diversity and Development of a SCAR Marker for Green Tea (Camellia sinensis) Cultivars in Zhejiang Province: The Most Famous Green Tea-Producing Area in China. Biochemical Genetics, 2019, 57, 555-570.	0.8	10
160	Light, but Not Nutrients, Drives Seasonal Congruence of Taxonomic and Functional Diversity of Phytoplankton in a Eutrophic Highland Lake in China. Frontiers in Plant Science, 2020, 11, 179.	1.7	10
161	Chemisorption of small fullerenes <mml:math inline"="" xmins:mml="http://www.w3.org/1998/Math/Math/Math/Math/Math/Math/Math&lt;br&gt;display="><mml:mrow><mml:msub><mml:mtext>C</mml:mtext><mml:mi>n</mml:mi></mml:msub><!--<br-->xmlns:mml="http://www.w3.org/1998/Math/MathML"</mml:mrow></mml:math>	mml:mrow:	>

#	Article	IF	CITATIONS
163	Solvothermal synthesis of hierarchical Eu <sub>2</sub> O <sub>3</sub> nanostructures templated by PS-b-PMAA: morphology control via simple variation of water contents. Journal of Materials Chemistry A, 2015, 3, 5789-5793.	5.2	7
164	Na Superionic Conductor-Type TiNb(PO <sub>4</sub> ) <sub>3</sub> Anode with High Energy Density and Long Cycle Life Enables Aqueous Alkaline-Ion Batteries. ACS Applied Materials & Interfaces, 2019, 11, 39757-39764.	4.0	7
165	Cloning and expression patterns of VQ-motif-containing proteins under abiotic stress in tea plant. Plant Growth Regulation, 2019, 87, 277-286.	1.8	7
166	Facile Synthesis of Amineâ€functionalized MOFs Incorporated Polyimide MMMs with Enhanced CO <sub>2</sub> Permselectivity. ChemistrySelect, 2019, 4, 2368-2373.	0.7	7
167	Ultra-small RuO2 nanoparticles supported on carbon cloth as a high-performance pseudocapacitive electrode. Advanced Composites and Hybrid Materials, 2022, 5, 696-703.	9.9	7
168	A first-principles study of CO oxidation by surface oxygen on Pt-incorporated perovskite catalyst (CaPt <sub>x</sub> Ti <sub>1â^'x</sub> O <sub>3</sub> ). RSC Advances, 2014, 4, 30530-30535.	1.7	5
169	Porous titania/carbon hybrid microspheres templated by in situ formed polystyrene colloids. Journal of Colloid and Interface Science, 2016, 469, 242-256.	5.0	5
170	Modulation of the inflammatory tumor microenvironment: a new approach for photothermal-synergized cancer immunotherapy. Nanomedicine, 2019, 14, 2101-2104.	1.7	5
171	Iron Hexcyanoferrate Nanocubes as Low-Strain Cathode Materials for Aqueous Li/Na Mixed-Ion Batteries. ACS Applied Nano Materials, 2020, 3, 1318-1323.	2.4	5
172	TRIM28 attenuates Bortezomib sensitivity of hepatocellular carcinoma cells through enhanced proteasome expression. Clinical and Translational Medicine, 2022, 12, e603.	1.7	5
173	Inhibition of AMPK activity by TRIM11 facilitates cell survival of hepatocellular carcinoma under metabolic stress. Clinical and Translational Medicine, 2021, 11, e617.	1.7	5
174	N-Carbamoylglutamate Supplementation on the Digestibility, Rumen Fermentation, Milk Quality, Antioxidant Parameters, and Metabolites of Jersey Cattle in High-Altitude Areas. Frontiers in Veterinary Science, 2022, 9, 848912.	0.9	4
175	Electrocatalysts: Ultrafine Defective RuO <sub>2</sub> Electrocatayst Integrated on Carbon Cloth for Robust Water Oxidation in Acidic Media (Adv. Energy Mater. 35/2019). Advanced Energy Materials, 2019, 9, 1970136.	10.2	3
176	Understanding the CO <sub>2</sub> /CH <sub>4</sub> /N <sub>2</sub> Separation Performance of Nanoporous Amorphous Nâ€Doped Carbon Combined Hybrid Monte Carlo with Machine Learning. Advanced Theory and Simulations, 2022, 5, 2100378.	1.3	3
177	A mechanistic study of CO removal on a small H-saturated platinum cluster. Science in China Series B: Chemistry, 2008, 51, 1187-1196.	0.8	2
178	Dietary amylose/amylopectin ratio influences the expression of amino acid transporters and enzyme activities for amino acid metabolism in the gastrointestinal tract of goats. British Journal of Nutrition, 2021, , 1-31.	1.2	2
179	Transition Metal Nanostructures: Formation and Stability of Low-Dimensional Structures for Group VIIIB and IB Transition Metals: The Role of sd4 Hybridization (Adv. Sci. 4/2016). Advanced Science, 2016, 3,	5.6	1
180	Collection of charge in NMOS from single event effect. IEICE Electronics Express, 2016, 13, 20160014-20160014.	0.3	1

#	Article	IF	CITATIONS
181	Generalized coefficient strengthening cuts for mixed integer programming. Journal of Global Optimization, 2018, 70, 289-306.	1.1	Ο
182	Effect of alfalfa substituted with ramie on the expression of apoptotic genes in the gastrointestinal tracts of goats. Food Science and Nutrition, 2022, 10, 2400-2407.	1.5	0